

УДК 548.2

**TAILORING OF OPTICAL AND MECHANICAL PROPERTIES OF HIGH-ENTROPY
CERAMIC THIN FLMS PREPARED BY HIPIMS SPUTTERING**

V.A. Bulakh, A.S. Mitulinsky

Scientific Supervisor: Dr. S.P. Zenkin

Tomsk Polytechnic University, Russia, Tomsk, Lenin str., 30, 634050

E-mail: vab67@tpu.ru

**ОПТИМИЗАЦИЯ ОПТИКО-МЕХАНИЧЕСКИХ СВОЙСТВ ВЫСОКОЭНТРОПИЙНЫХ
ПЛЕНОК КЕРАМИКИ, ИЗГОТОВЛЕННЫХ МЕТОДОМ HIPIMS НАПЫЛЕНИЯ**

В.А. Булах, А.С. Митулинский

Научный руководитель: PhD, в.н.с. С.П. Зенкин

Национальный исследовательский Томский политехнический университет,

Россия, г. Томск, пр. Ленина, 30, 634050

E-mail: vab67@tpu.ru

***Аннотация.** Был проведен синтез высокоэнтропийных тонких пленок Hf-Zr-Ce-Y-O и определены их оптические и механические свойства в зависимости от состава. Hf₄Zr₄CeY₂O₂₁ показывает до трех раз более высокую твердость по сравнению с двойным оксидом HfZrO₄ и до 50 % более высокую твердость по сравнению с кубическими ZrO₂ и HfO₂. Эквимолярные пленки обладают высоким коэффициентом пропускания >85 % и твердостью до 20 ГПа.*

Introduction. The conception of the entropy stabilization of the solid crystal structure has received a wide attention in the past decade due to superior and tunable properties of reported high entropy materials. High entropy alloys are surpassing traditional alloys and compounds in thermal stability and mechanical properties, making them a potential high-performance constructive and functional material [1]. A high entropy material is a solid solution of four-, five- or more components with a simple crystal structure, usually BCC or FCC.

An entropy of the system is described using the Boltzmann's equation:

$$\Delta S_{mix} = -R \sum c_i \ln(c_i) \quad (1)$$

Here, R is the gas constant, and c_i is the molar content of the component.

Resulted Gibbs free energy from the Eq. (1) is minimized by the enlarged entropy of mixing with the value up to $\Delta S_{mix} = 1.61R$ for five-component materials in comparison with traditional materials, giving an additional thermodynamic stabilization of the system. This remarkable improvement of material properties led to the suggestion that entropic stabilization is also applicable for the UHTC ceramics production, where the reduced Gibbs free energy can lead to the higher thermal stability of solids. In order to create a robust transparent ceramics for the selection of the high entropy oxide (HEO) composition we used the combination of three material properties: a high melting temperature of the oxide, the lowest enthalpy of formation (or minimum Gibbs free energy per mole O₂) and low electronegativity of the base element [2]. A resulting group of selected oxides included HfO₂, ZrO₂, Y₂O₃ and CeO₂, - and excluded radioactive ThO₂, PuO₂, and toxic BeO (Fig. 1a).

The obtained composition of HEO $\text{HfZrCeYO}_{2-\delta}$ is characterized by the entropy value $\Delta S_{\text{mix}} = 1.38R$ and a simple cubic Fm-3m structure (Fig. 1b).

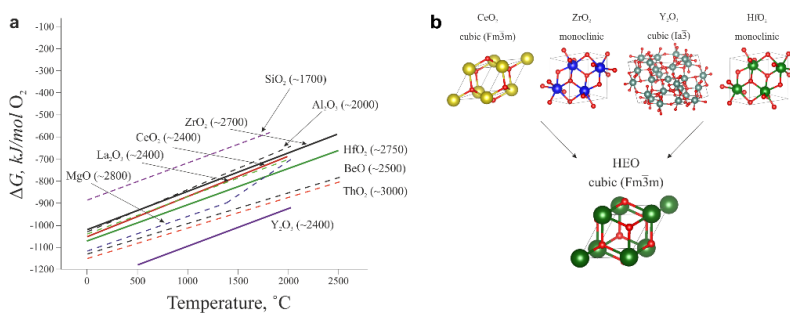


Fig. 1. Ellingham diagrams of the most thermally stable oxides with respective melting temperatures (a); crystal structures of the selected component oxides at the ambient conditions and resulting crystal structure of the high entropy oxide $\text{HfZrCeYO}_{2-\delta}$ (b)

Experimental part. High entropy oxide films were sputtered using two round unbalanced magnetrons equipped with HfZr (50/50 at. %) and CeY (33/66 at. %) targets. Coatings surface, cross-sectional morphology and elemental composition were studied using a scanning electron microscope. Structural characteristics of the coatings were studied using X-ray diffraction with $\text{Cu K}\alpha$ ($\lambda = 0.154$ nm) radiation. Samples curvature was measured by the optical proflometer and film stress was calculated from the curvature measurements by using the Stoney formula.

Results. Firstly, to compare properties we prepared binary $\text{Ce}_3\text{Y}_4\text{O}_{12}$ and HfZrO_4 films, as shown in Fig. 2a. Sputtered binary oxides are characterized by the cubic structure for $\text{Ce}_3\text{Y}_4\text{O}_{12}$ and the mixed cubic + monoclinic structure for HfZrO_4 without preferred orientation (Fig. 2a, blue and orange lines respectively).

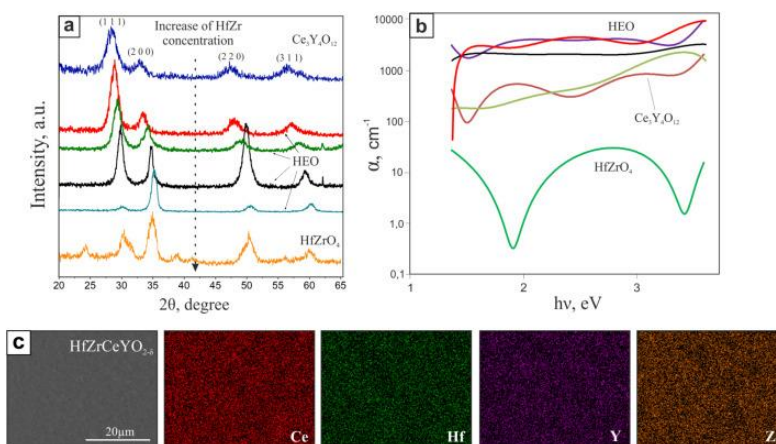


Fig. 2. XRD patterns of synthesized HEO films (a); Spectral dependence of the absorption coefficient of HEO films (b); top view SEM of the $\text{Hf}_2\text{Zr}_2\text{CeY}_2\text{O}_{13}$ and the corresponding EDS mapping (c)

On the contrary, HEO films are characterized by the cubic Fm-3m structure with XRD peaks shifted proportionally to the increase of the molar HfZr concentration in agreement with the Vegard's law. The obtained 2θ peak shift is in the range of 1.29° for (1 1 1) and up to 3.06° for (3 1 1). The preferred orientation of sputtered HEO films is transformed from (1 1 1) to (2 0 0) plane with the growth of the HfZr concentration.

A cubic Fm-3m structure of $\text{HfZrCeYO}_{2-\delta}$ does not divide to separated mono- or binary oxides in a wide range of molar compositions. EDS mapping of the representative $\text{Hf}_2\text{Zr}_2\text{CeY}_2\text{O}_{13}$ film shows the homogeneous

distribution of all constituent elements without any local elements segregation and phase separation to the Me-rich regions, (Fig. 2c) HfZrO₄ films are characterized by the minimum of the light absorption centers concentration for all synthesized films with the characteristic absorption value around 2.8 eV, due to the ordered crystalline structure. Contrary, Ce₃Y₄O₁₂ exhibited in order of magnitude higher value of light absorption centers concentration. A transfer from the Ce₃Y₄O₁₂ to the HfZrO₄ by an addition of the HfZr is characterized by the formation of HfZrCeYO_{2-δ} composition with a higher absorption centers concentration, leading to the growth of the absorption coefficient in order of magnitude. Distribution of these centers is homogeneous for the whole measurement interval for HfZrCeYO_{2-δ} compositions from HfZrCeY₂O₉ to Hf₄Zr₄CeY₂O₂₁. For the light wavelength of 550 nm the transmittance of the 2800 nm thick Hf₂Zr₂CeY₂O₁₃ film is around 85 % while for 500 nm thick Hf₂Zr₂CeY₂O₁₃ film transmittance is around 90 %, that is comparable with an uncoated glass substrate.

Table 1

Mechanical properties of the synthesized HfZrCeYO_{2-δ} films

Elemental composition	H [GPa]	E* [GPa]	W _e [%]	H/E*	σ [GPa]
Ce ₃ Y ₄ O ₁₂	4,9	79,3	60	0,062	-0,5
Hf _{0,5} Zr _{0,5} CeY ₂ O ₇	17,3	180,6	66	0,096	-0,7
HfZrCeY ₂ O ₉	19,7	187,6	67	0,105	-0,9
Hf ₂ Zr ₂ CeY ₂ O ₁₃	21,3	196,7	69	0,108	-1,3
Hf ₄ Zr ₄ CeY ₂ O ₂₁	22,4	194,8	71	0,115	-1,2
HfZrO ₄	7,7	110,3	62	0,070	-0,9

The mechanical properties of as-prepared HfZrCeYO_{2-δ} films are summarized in Table 1. All the films exhibited a relatively low residual compressive stress σ less than -1,5 GPa and a high elastic recovery W_e > 60 %. Hardness H and Young's modulus E* continuously increase with the shift from binary oxides Ce₃Y₄O₁₂ and HfZrO₄ to the equimolar HfZrCeYO_{2-δ} composition with a maximum hardness of H = 22.4 GPa for the Hf₄Zr₄CeY₂O₂₁. Also, for the HfZrCeYO_{2-δ} film group HfZrCeY₂O₉ - Hf₄Zr₄CeY₂O₂₁ one can detect a high ratio of H/E* > 0.1, which is in combination with a high elastic recovery W_e > 60 % gives an enhanced resistance to cracks formation. HfZrCeYO_{2-δ} shows up to three times higher hardness in comparison with binary HfZrO₄ oxide and up to 50 % higher hardness in comparison with cubic ZrO₂ and HfO₂.

Conclusion. Based on the measured data we can conclude that:

- 1) The HfZrCeYO_{2-δ} system form a solid solution with the simple cubic (Fm-3 m) structure without formation of binary oxides and an absence of the phase separation.
- 2) Hardness in the Hf-Zr-Ce-Y-O system shows nonlinear character in behavior, depending on the molar composition. Hf₄Zr₄CeY₂O₂₁ shows up to three times higher hardness (H = 22GPa) in comparison to binary HfZrO₄ oxide and up to 50 % higher hardness in comparison with cubic ZrO₂ and HfO₂ due to the solid solution hardening effect.

REFERENCES

1. Zenkin S., Gaydaychuk A., Mitulinsky A., Linnik S., Tailoring of optical, mechanical and surface properties of high-entropy Hf-Zr-Ce-YO ceramic thin films prepared by HiPIMS sputtering // Surface and Coatings Technology. – 2022. – Vol. 433. – P. 128164.
2. Fahrenholtz W.G., Hilmas G.E. Ultra-high temperature ceramics: materials for extreme environments Scr. Mater., no. 129 (2017), pp. 94-99. doi:10.1016/j.scriptamat.2016.10.018